Arresting UV-Laser Damage in Fused Silica

Deciding when to replace spot-damage-afflicted fused-silica optics or, in the case of inaccessible, space-based lasers, predicting the useful service life of fused-silica optics before catastrophic, pulsed-laser-driven crack growth shatters a part has recently become simpler. By empirically deriving a rule for laser-driven crack growth in fused silica as a function of the number of constant-fluence laser pulses, Dahmani *et al.*[1] provided laser systems designers and operators with guidance on the crack-growth kinetics as well as on the stress-related ramifications such a laser-driven crack entails. Specifically, a *hoop stress* in the immediate vicinity of a crack growing along the beam propagation direction was identified as strongly coupling to both the laser fluence and the crack.[2] It prompted the question of whether or not *breaking the hoop-stress symmetry* by some external perturbation will accelerate or stymie crack growth or, alternatively, will have no effect at all.

In this article, we report not only on the finding that, depending on the *magnitude* of a perturbing external stress, crack propagation in fused silica may *slow* relative to stress-free conditions, but also the more unexpected finding that the applied external stress *raises the damage-initiation fluence*. In gathering this evidence, a conventional experimental arrangement was used.

Pulses from a Nd:glass oscillator/single-pass amplifier system were frequency tripled in a dual-crystal KDP cell to yield temporally stable, 500-ps pulses at a repetition rate of one pulse every 10 s. Prior to frequency conversion, the IR pulse was sent through a nonmagnifying, vacuum spatial filter. UV pulses were focused by a 2-m-focal-length lens to an ~600-μm spot size at the sample entrance surface. For each pulse, a record of the fluence distribution in this spot was acquired by a charge-injection-device camera located in a sample-equivalent plane and digitized to 8-bit accuracy. Spatially integrated UV energy per pulse was also monitored on each exposure. The UV beam-incidence direction was chosen to be a few degrees (<10) off-normal to the sample entrance face to prevent (1) any back-reflection of residual, unconverted IR from seeding the amplifier in the backward direction, and (2) setting up a 351-nm interference pattern between sample entrance and exit surfaces that would invalidate the calculated fluence distribution. Damage initiation anywhere between the two sample surfaces, i.e., along the pulse-propagation direction, was recorded by 110×-magnification dark-field microscopy. After damage initiation, the crack length was measured microscopically by viewing the sample *orthogonally* to the laser-pulse propagation direction.

Fused-silica samples (Corning 7940, UV Grade A), with length L = 64 mm, width w = 13.6 mm, and thickness t = 4.6 mm, were conventionally pitch polished to *laser quality* on the entrance and exit surfaces and to *cosmetic quality* around the edges.

Samples were mechanically stressed by first centering each between apertured aluminum plates separately attached to a load cell (Eaton, Model 3397-25, maximum load capacity: 25 lbs). A predetermined, constant, uniaxial, compressive load was applied in such a manner that the compressive-force direction nearly coincided with the laser-pulse propagation direction (Fig. 77.26). The laser pulse entered and exited the samples through the apertures in the aluminum plates. The need for having beam-passage apertures *ipso facto* brings about stress conditions that vary from point to point within the aperture, both in magnitude and in principal directions (compressive or tensile). At first, this may appear as complicating data interpretation; for the following reason, however, it does not.

Laser-damage thresholds (for pulse lengths greater than picoseconds) are always reported as *average values* derived from a statistical number of sample sites *per tested specimen*. In all *nondeterministic*, i.e., extrinsic-impurity-driven, laser-damage processes the occurrence of damage hinges on the statistical presence or absence of one or more absorbing impurities within a given irradiated area. This statistical distribution in defect volume density is now convoluted by a site-to-site–varying stress distribution. In an ideal experiment, a large enough number of tests on samples and sites with precisely

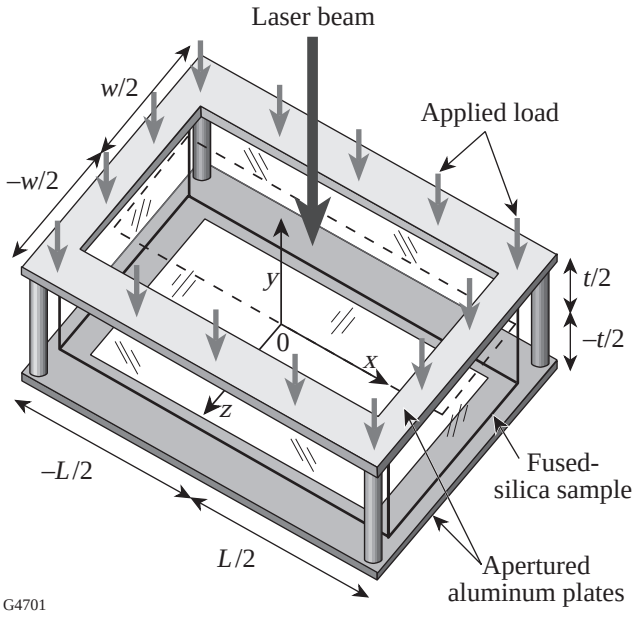

Figure 77.26
Experimental arrangement for applying compressive loads to fused-silica surfaces by clamping the conventionally polished sample between aluminum plates. The static pressure applied is measured by the load cell. Sample dimensions are length L = 64 mm, width w = 13.6 mm, and thickness t = 4.6 mm oriented relative to the Cartesian coordinate system as indicated.

known local stress will deconvolve the two distributions; in practice, however, this is unrealistic. Rather, simulation of local stress conditions by finite-element methods,[3] or when possible by analytic approaches, permits one to find with acceptable accuracy, for various aperture boundary conditions, the compressive and tensile stresses within the aperture, based on which one may choose many irradiation sites on a single sample. To guarantee good statistics, however, the current measurements still rely on more than one sample. All stress values quoted here are numerically derived from experimentally measured sample-loading conditions. The total applied force on the sample is 10 kgf (1 kgf = 9.8 N) in this case.

The onset of damage is defined as follows: for the given microscopic magnification and lighting conditions, any observable, permanent, irradiation-induced, surface or bulk modification. Throughout this article, initiation thresholds are reported for *1-on-1 mode*, i.e., each sample site is irradiated only once. For well-known reasons,[4] conventionally polished material of good bulk purity damages first at the exit surface. In these experiments, this is not only confirmed but *damage propagation* effects under multiple irradiation conditions are, for now, deliberately restricted to those events in which throughout *damage-crack initiation and growth* no entrance-surface damage is encountered, i.e., the laser fluence at the damage site remains unobscured by upstream obstacles.

We first report the effect of stress on *damage initiation*. In Fig. 77.27, the 351-nm, damage-onset fluence threshold is plotted for exit-surface damage (× symbols) against applied stress magnitude (sign convention: + tensile, – compressive). Here the load is applied nearly collinear with the pulse-propagation direction. As is immediately evident, regardless of whether the stress character is tensile or compressive, *threshold enhancements* of up to 70% are attainable from modest stresses, and the largest, relative threshold-improvement increments can be garnered from the smallest stresses. Note how the symmetry around zero stress tends to imply that the underlying damage-initiation process is independent of whether the stress is compressive or tensile. Over how large a tensile-stress range this holds true is yet to be ascertained.

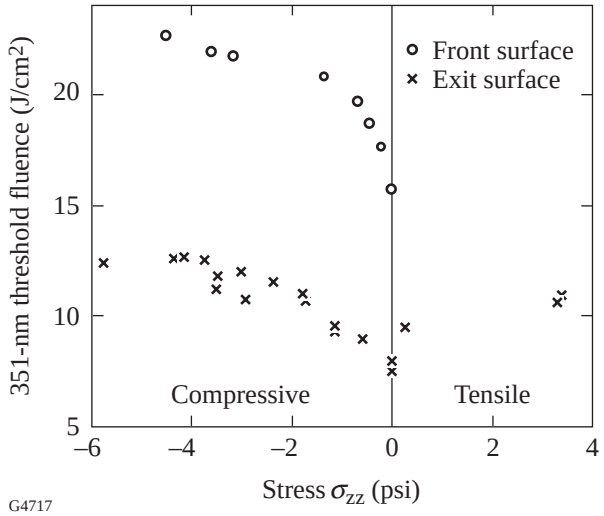

Figure 77.27
Entrance (*x*)- and exit (*o*)-surface, 351-nm damage-*initiation* threshold as a function of applied stress follows similar trends.

For the laser systems designer it is important to know if the beneficial stress effect is an *exit-surface phenomenon only* or if an equivalent advantage can be gained for the entrance surface as well. Collecting the data for which *front-surface damage* was incurred, i.e., data excluded so far, Fig. 77.27 also plots a similar trend for the entrance-surface damage-initiation threshold (open circles) as for the exit surface.

We next concentrate on *laser-driven crack growth.* Once the exit-surface damage-initiation threshold $F_{\text{exit/thr}}$ is determined as described above, a *flaw* is deliberately created at a

new site, which upon further irradiation becomes the source for both crack formation and crack propagation. Cracks observed in these experiments are not empty voids but are filled with granular glass debris that scatters light efficiently. The growth dynamics of such cracks as a function of incident fluence and number of exposures has already been reported elsewhere.[2] To underscore the influence of stress on the crack-growth kinetics, we compare here results obtained under extreme conditions, i.e., for irradiation of a flaw by 270 consecutive laser pulses of constant fluence $F_L = 2.1 \times F_{\text{exit/thr}}$, a far-from-normal condition for most lasers. By choosing extreme irradiation conditions, *crack-growth arrest* is most convincingly demonstrated. Figure 77.28 displays side-by-side micrographs of cracks formed in (a) the unstressed sample ($\sigma_{zz} = 0$) and (b) the stressed sample ($\sigma_{zz} = -6$ psi). Note that in Fig. 77.28(a) the crack growth has pushed the crack tip beyond the field of view. A less-striking, though quantitative, account of crack arrest as a function of applied stress is displayed in Fig. 77.29, where the length of cracks from multiple sites, all irradiated at the above-fluence condition, is plotted against the stress prevailing at any particular site. The functional dependence on applied stress displayed in Fig. 77.29 offers promise: much can be achieved in altering, by modest stress, the crack-propagation outcome, while the empirical crack-length-reduction *limit* for larger stresses renders these unnecessary in practice. The concomitant penalty in stress-induced birefringence that such crack-growth prevention entails is also kept within bounds: the maximum stress of 6 psi plotted in Figs. 77.27 and 77.29 causes 0.5-nm retardance. A second, intriguing ramification of the slope in Fig. 77.29 pertains to damage testing in general: there exists evidence[5] that the polishing process leaves a thin, densified layer of silica at/near the air interface, the stress within which may locally vary or may vary from sample to sample. Depending on the extent of such variation, the statistical error on measured surface-damage initiation thresholds should correspondingly be large since the slope in Fig. 77.27 is steepest near zero stress. An unfortunate paucity of reported 351-nm, fused-silica, surface-damage thresholds makes it, at this time, difficult to corroborate this correlation from literature data. In the same vein, there should be a damage-initiation stress effect for interfacial damage on *coated* or *cladded* silica surfaces whenever the thermal-expansion mismatch between the substrate and the film stack or cladding material introduces interfacial stress. This would be most readily observable in antireflective coatings as these permit significant laser intensity to reach the substrate interface. Finally, there remains an urgent question to be resolved as to whether this phenomenon is unique to fused silica or may be present also in other glasses.

We presented here results from stress-inhibited laser-driven crack propagation and stress-delayed damage-initiation experiments in fused silica at 351 nm. Within the stress interval of $-6 \le \sigma_{zz} \le 4$ psi, the damage initiation threshold is raised by

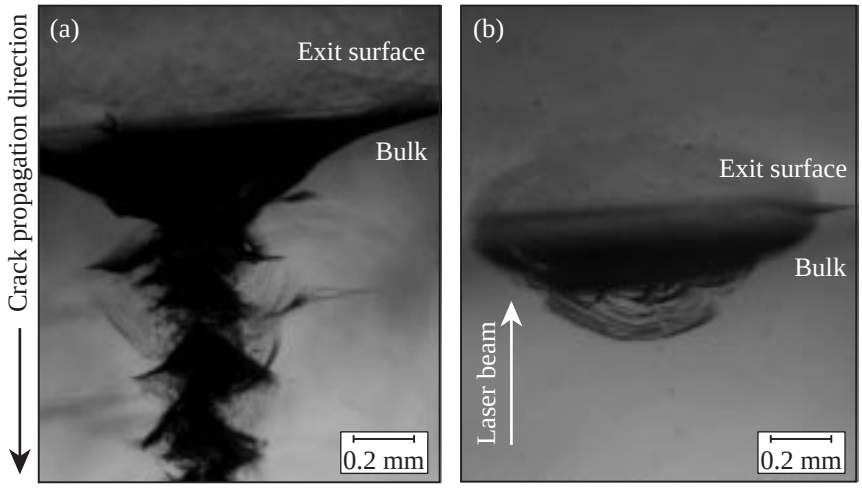

Figure 77.28
Cross-sectional micrographs of laser-induced cracks after 270 exposures to constant fluences $F_L = 2.1 \times F_{\text{exit/thr}}$ in (a) a sample free of external stress and (b) a sample with $\sigma_{zz} = -6$ psi. The crack tip in micrograph (a) is, for the given magnification, located already outside the field of view.

70%. For such modest stresses, both compressive or tensile stresses appear to raise this threshold while keeping the induced-birefringence penalty ≤0.5-nm retardation. The ramifications of these findings for large-aperture systems, such as OMEGA, are yet to fully emerge: aperture scaling must commence and the stress-magnitude regime must be extended to higher stresses in order to evaluate whether or not the apparent saturation (near-zero slope) at 6 psi remains. These tasks are in progress at this time.

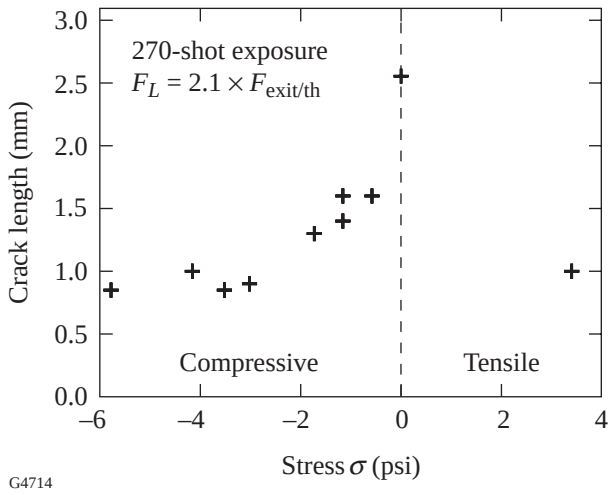

Figure 77.29
Crack length as a function of applied external stress for identical irradiation conditions as in Fig. 77.28.

ACKNOWLEDGMENT

This project was funded by the U.S. Department of Energy under Cooperative Agreement No. DE-FC03-92SF19460, the University of Rochester, and the New York State Energy Research Development Authority. The support of DOE does not constitute an endorsement of the views expressed in this article. One of the authors thanks the Laboratory for Laser Energetics for an F. J. Horton Fellowship. We thank Alex Maltsev for masterfully polishing all sample faces and Tom Greene for loan of the load cell.

REFERENCES

1. F. Dahmani, J. C. Lambropoulos, A. W. Schmid, S. Papernov, and S. J. Burns, "Fracture of Fused Silica with 351-nm-Laser-Generated Surface Cracks," to be published in Journal of Materials Research.
2. F. Dahmani, A. W. Schmid, J. C. Lambropoulos, and S. J. Burns, Appl. Opt. **37**, 7772 (1998).
3. ANSYS 5.4® is a finite-element code developed by Ansys Inc.
4. N. L. Boling, M. D. Crisp, and G. Dubé, Appl. Opt. **12**, 650 (1973).
5. H. Yokota *et al.*, Surf. Sci. **16**, 265 (1969).